



When the velocity of rotating mass comes close to zero, this value significantly changes due to nonlinear and varying characteristics of friction coefficients. This causes the decrease of accuracy in the motion control systems and is a reason for difficulty in handling it via a linear control method.

2. Stick-Slip friction phenomena

The stick-slip friction force model which is a modification of the model introduced by Karnopp[5] allows for the evaluation of the friction force during sticking and slipping motions in the mechatronics system. This also eliminates the numerical problems associated with near zero -velocity force computation. The stick-slip friction model is obtained by Eq. (2) only in the limit as  $a \rightarrow 0$ .

$$F = F_{slip}(\dot{x})I(\dot{x}) + F_{stick}(t)[1 - I(\dot{x})] \tag{2a}$$

where,

$$I(\dot{x}) = \begin{cases} 1, & |\dot{x}| > a > 0 \\ 0, & |\dot{x}| \leq a < 0 \end{cases} \tag{2b}$$

Throughout the analytical investigation, the artificial zero parameter,  $a$ , is taken to be identically zero. Nonzero values are only used in the simulation purpose to insure that numerical integration algorithm remains to be stable.

The stick friction may be represented by Eq. (3).

$$F_{stick}(t) = \begin{cases} F_s^+ & t(t) \geq F_s^+ > 0 \\ t(t) & F_s^- < t(t) < F_s^+ \\ F_s^- & t(t) \leq F_s^- < 0 \end{cases} \tag{3}$$

The above sticking friction provides the values of the friction force at the zero velocity (or near zero velocity).

This friction is just regarded a dead zone to determine whether the moving mass will stick or break free from the static friction forces. The positive and negative limits on the static friction forces are given by  $F_s^+$  and  $F_s^-$ , respectively. The static friction force limits are assumed to be constant in this analysis. When the moving mass does not move i.e.,  $\dot{x} = 0$ , and the applied force is between the static levels, the damping mechanism provides a force which keeps the mass at rest. This means that the moving mass cannot move until the applied force is greater in magnitude than the respective static force. The sticking force is shown on Fig. 3.

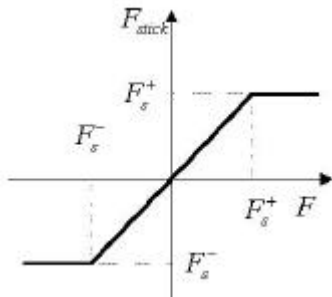


Fig. 3. Stick friction model.

2.3 Slip friction analysis

The slipping friction provides values of the friction forces at

nonzero velocity represented by Eq. (4).

$$F_{slip}(\dot{x}) = F_d^+(\dot{x})m(\dot{x}) + F_d^-(\dot{x})m(-\dot{x}) \tag{4}$$

where,

$$m(\dot{x}) = \begin{cases} 1 & \dot{x} > 0 \\ 0 & \dot{x} \leq 0 \end{cases} \tag{5}$$

$$F_d^+ = F_s^+ - \Delta F^+ [1 - e^{-(\dot{x}/\dot{x}_{CR}^+)}] + B^+ \dot{x} \tag{6a}$$

$$F_d^- = F_s^- - \Delta F^- [1 - e^{-(\dot{x}/\dot{x}_{CR}^-)}] + B^- \dot{x} \tag{6b}$$

where  $\Delta F_s^+$  and  $\Delta F_s^-$  are respective force drops from the static to kinetic force level,  $\dot{x}_{CR}^+$  and  $\dot{x}_{CR}^-$  are the critical Stribeck velocity[6], and  $B^+$  and  $B^-$  are the positive and negative viscous friction coefficients, respectively. This friction force is composed of the Coulomb friction, viscous friction, and the Stribeck effect. The positive and negative Coulomb friction level is respectively presented as  $F_c^+ = F_s^+ - \Delta F^+$  and  $F_c^- = F_s^- - \Delta F^-$ . The Stribeck effect is that the friction force is in many cases decreasing with increased relative velocity[4]. It is caused by increased fluid lubrication. An example of the slipping friction force is shown in Fig. 4.

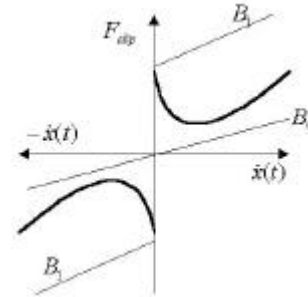


Fig. 4. Slip friction model.

The slipping friction force is assumed to dissipate energy at all the nonzero velocities, and therefore is bounded within the first and third quadrants. It is assumed there exist constants.

$$B_1 > \max(B^+, B^-) \tag{7a}$$

$$F_0 \geq \max(|F_s^+|, |F_s^-|), \quad F_0 > 0 \tag{7b}$$

which define the piecewise linear bound for the slipping friction forces as shown Fig. 4.

$$F_d^+(\dot{x}) \leq F_0 + B_1 \dot{x}(t), \quad \forall \dot{x}(t) > 0 \tag{8a}$$

$$F_d^-(\dot{x}) \geq -F_0 + B_1 \dot{x}(t), \quad \forall \dot{x}(t) < 0 \tag{8b}$$

Therefore, we can assume that the slip friction is bounded within a linear bound.

$$|F_{slip}(\dot{x})| \leq F_0 + B_1 |\dot{x}(t)|, \quad \forall \dot{x}(t) \tag{9}$$

III. Friction compensation

With the nonlinear friction characteristics of the mechanism described above, even if a good physical model of the nonlinear system could be obtained, it is often difficult to predict the

friction force to compensate it correctly in the linear control system since the dynamics near the region of zero velocity are dominated by the nonlinear and discontinuous functions. If nonlinear phenomena exist that are unknown to the designer, the problem to design high accuracy motion control systems is even more difficult. In many practical motion control systems, there are no means to estimate the nonlinear friction accurately and to compensate it effectively.

As a result, they are of poor accuracy and may cause the limit cycles near zero velocity.

1. Design strategy

In literature, many control techniques have been proposed for friction compensation [1]-[8]. However, they still have some questions to realize it in the mechatronics industry. In this work, we shall propose usage of a more realistic supplementary friction compensator to the currently available control system so that the overall control performance is guaranteed. By observing Fig.1 the nonlinear friction force may be compensated by adding an appropriate compensating term to the control action, i.e.,

$$u(t) = u_r(t) + u_c(t) \tag{10}$$

where  $u_r(t)$  is normal position and velocity controller output based on the linear system, whereas  $u_c(t)$  is friction compensator output which is to cancel the nonlinear friction phenomena.

The normal position and velocity controller has traditionally been used in the motion control servo systems represented by Eq. (11) and (12). Let  $x_d(t)$  be desired trajectory and we define

$$e(t) = x_d(t) - x(t) \text{ or } e(t) = q_{ref}(t) - q(t) \tag{11a}$$

$$\dot{e}(t) = \dot{x}_d(t) - \dot{x}(t) \text{ or } \dot{e}(t) = K_p e(t) - w(t) \tag{11b}$$

$$u_r(t) = K_v \dot{e}(t) + \frac{1}{T_i} \int_0^t \dot{e}(t) dt \tag{12}$$

where  $K_p$ ,  $K_v$ ,  $T_i$  are proportional gain of position loop and velocity loop and integral time constant of velocity loop, respectively. Eq. (12) indicates that the position control loop has the proportional term only and velocity control loop consists of proportional and integral terms as they are traditionally available in most motion control servo systems. Instead, we shall propose an adaptive neural network compensator for the friction compensator to be fed-back positively to the torque control loop.

2. Neural Network Compensator Design

We approached a nonlinear mapping between input,  $x_i$ , and output,  $y_i$ , of neural network under the assumption that the actual nonlinear function is unknown. The input-output of a neural network may be described by Eq. (13) and (14);

$$y_i = f(s_i) \tag{13}$$

$$s_i = \sum_j^n w_{ij} x_j + b_i \tag{14}$$

where  $f(s)$  is the activation function, and  $w_{ij}$ ,  $b_j$  are connection weighting values and bias values of each neuron, re-

spectively. The connection weight between the  $i$ -th neuron in the  $(l-1)$  th layer and  $j$ -th neuron in the  $l$ -th layer,  $w_{ij}^l$ , at each learning step may be adjusted by the error back-propagation learning rule [8] as follows;

$$E = \frac{1}{2} (d - y)^T (d - y) \tag{15}$$

$$w_{ij}^l(k+1) = w_{ij}^l(k) + h \Delta w_{ij}^l \tag{16}$$

$$\Delta w_{ij}^l = \frac{\partial E}{\partial w_{ij}^l} \tag{17}$$

where  $E$  is a sum of square error between network output,  $y_i$ , and its desired output (or target) vector,  $d$ , and  $h$  is a learning rate, respectively.

In our design, the input signals are selected as 5 time delayed sequences,  $\dot{x}(t), \dot{x}(t-1), \dot{x}(t-2), \dot{x}(t-3), \dot{x}(t-4)$  of velocity of plant output. Fig. 5 shows an adaptive neural network for this purpose of which the network consists of 5 hidden units and 1 output unit. The activation functions are considered hyperbolic tangents [9] for the hidden layer and pure linear function [9] for the output layer, respectively. The error back-propagation algorithm is chosen to train the neural network. In order to train the network, slip friction dynamics given by in Eq. (4), (5) and (6) is selected as a target function.

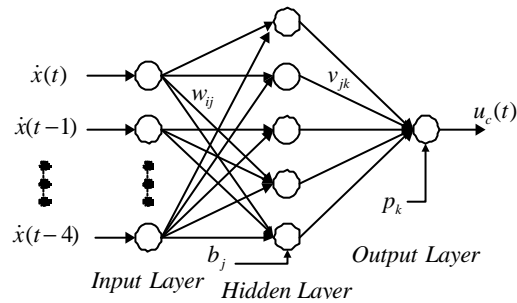


Fig. 5. Neural network model.

IV. Simulation results

1. Simulation conditions

A numerical simulation of the overall mechatronics servo system including a normal controller and a compensator was carried out to verify the compensation effects. In order to reflect a more realistic system, the X-Y positioning table was considered for this simulation. Signals from the position and velocity measurements were assumed to be quantized by 12-bits A/D converters. Based on laboratory calibrations of experimental sensors, it is reasonable to assume a resolution of 0.25mm for positioning and 1 cm/sec for velocity. Sampling time is 250 microseconds and zero-order-holder time delay is also considered. The parameters for this system are summarized in Table 1. The desired trajectory was applied for 2 cases as follows;

- a) Sinusoidal signals input to X-Y Axis Table.
- b) Step functioned pulse signals input to X-Y Axis Table.

The stick force works only at the starting time and changing direction time near zero velocity. This effect is too small to compensate the values. The slipping friction force is assumed

to exponentially decay from the static level to a kinetic friction force at higher velocity with viscous damping term added .

Table 1. Summary of simulation parameters [7]-[10].

Para.	Unit	Value	Para.	Unit	Value
$R_a$	$\Omega$	1.59	$K_p, K_V$	-, -	6,40
$L_a$	MH	1.27	$T_i$	sec	0.04
$J_m$	$\text{Kg.cm}^2$	0.235	$F^{+,-}$	N	3.8
$J_i$	$\text{Kg.cm}^2$	1.175	$\Delta F^{+,-}$	N	2.1
$K_t$	$\text{Kg.cm/A}$	7.54	$\Delta \dot{x}_{CR}^{+,-}$	m/s	0.2
$K_e$	mV/rpm	7.9	$B^{+,-}$	N/(m/s)	0.4
P	Watt	49.3	$a$	m/s	0.001

2. Simulation results

Training result of target slipping friction of adaptive neural network was just corresponded to friction modeled by Eq. (4), (5), (6) and Fig. 4.

The optimal weighting values and biasing values of two layers were obtained in the off-line learning process. The simulation results indicate the error between desired trajectory and actual positioning at the starting time and at the turning points of the direction of X-Y table movement is smaller than without a compensator (Fig. 6,7,10 and 11).

The velocity in X-Y Table with a neural network compensator is also responded to be a smaller deviation from the reference velocity than without a compensator (Fig. 8 and 12).

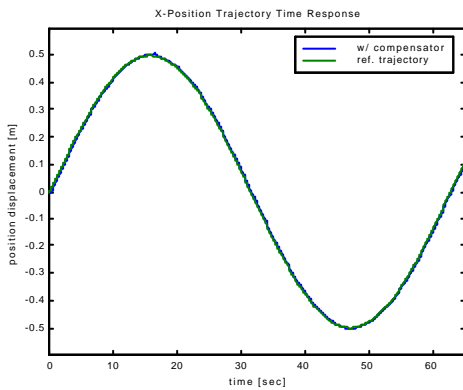


Fig. 6. X-position time response for case (a).

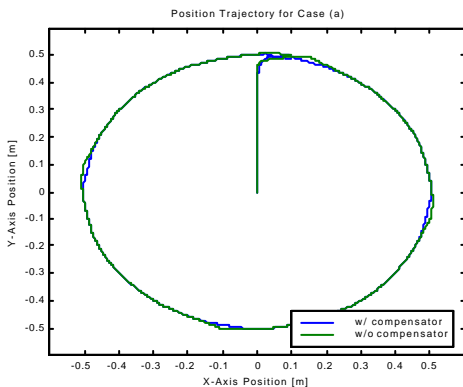


Fig. 7. Position responded trajectory for case (a) (w/ compensator; w/o compensator).

The neural network output for a friction compensator is very closely responded to the simulated slip friction force output, which cancels the slipping friction effects (Fig. 9 and 13).

3. Comparison with the laboratory experimental results

One of authors has experienced in the laboratory experiment that the slip friction occurred at the turning points of moving mass in the X-Y table and could improve the residual errors using an appropriate friction compensator as shown Fig. (14) and (15). These experimental results are very closely responded to those in the simulation of Fig.6.

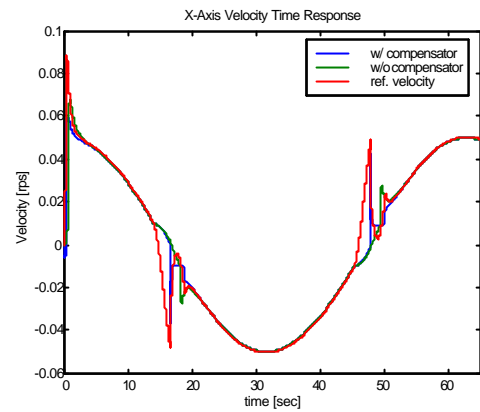


Fig. 8. Velocity time response (X-axis) for case (a). (Ref. Velocity; w/ compensator; w/o compensator).

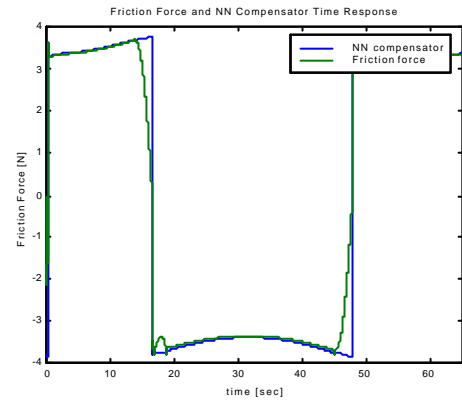


Fig. 9. Friction and NN compensator time response for case (a).

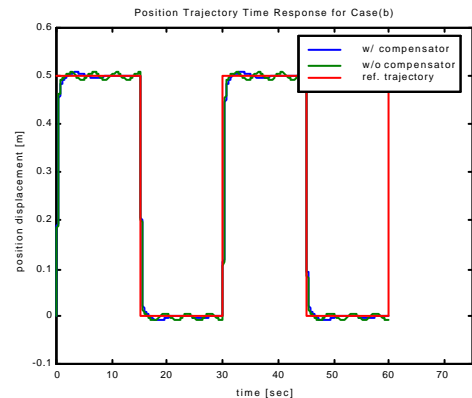


Fig. 10. X-position time response for case (b).

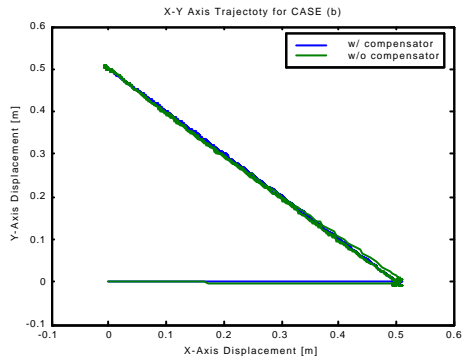


Fig. 11. Position responded trajectory for case (b) (w/ compensator; w/o compensator).

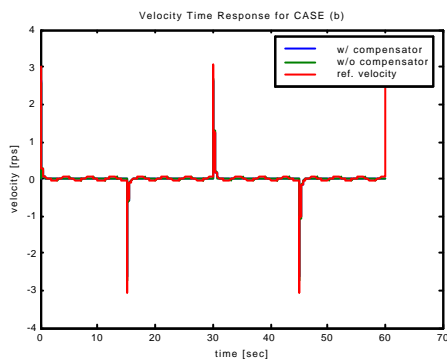


Fig. 12. Velocity time response (X-Axis) for case (b) (Ref. Velocity; w/ compensator; w/o compensator).

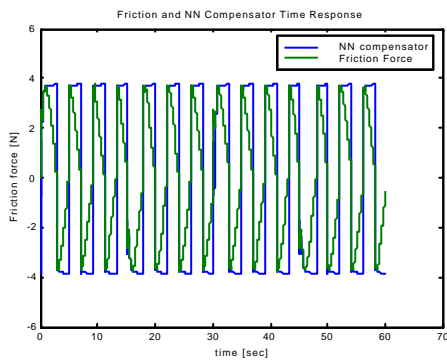


Fig. 13. Friction and NN compensator time response for case (b).

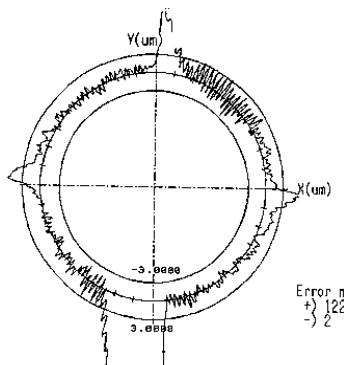


Fig. 14. Experimental record for Case (a) (X-Y Table w/o compensation).

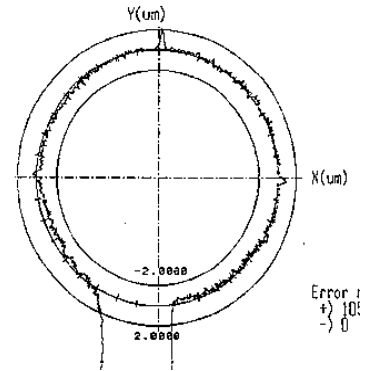


Fig. 15. Experimental Record for Case (a) (X-Y Table w/ compensation).

**V. Conclusion**

In our work, it was confirmed that poor accuracy due to the stick-slip friction takes place at the near zero velocity and at the turning points of moving direction. It can be overcome by the design of the supplementary compensator to the traditional position and velocity control loops. The neural network compensator is most appropriate for this purpose since it works effectively and can be easily implemented in the digital computer, making use of conventional position and velocity loop control primarily.

**VI. References**

- [1] S. W. Lee and J. H. Kim, "Robust adaptive stick-friction compensation," *IEEE Trans. on Industrial Electronics*, vol. 42, no. 5, pp. 474-479, Oct. 1995.
- [2] S. S. Ge, T. H. Lee, and X. Ren, "Adaptive friction compensation of servo mechanisms," *IEEE Proceedings on Control Application*, TuP4-3, pp. 1175-1180, Aug. 22-27, 1999.
- [3] C. G. Bario and P. O. Gutrman, "Performance enhancing adaptive friction compensation for uncertain systems," *IEEE Transactions on Control Systems Technology*, vol. 5, no. 5, pp. 466-479, Oct. 1997.
- [4] D. A. Haessig and B. Friedland, "On modeling and simulation of friction," *ASME Journal of Dynamics System, Measurement, and Control*, vol. 113, pp. 354-362, Sep. 1991.
- [5] D. Karnopp, "Computer simulation of stick-slip friction in mechanical dynamic system," *ASME Journal of Dynamics System, Measurement, and Control*, vol. 107, pp. 100-103, 1985.
- [6] K.C. Cheok, H.X Hu, and N. K. Loh, "Modeling and identification of servomechanism systems with stick-slip friction," *ASME Journal of Dynamics System, Measurement, and Control*, vol. 110, pp. 324-328, Sep. 1988.
- [7] Y.H. Kim and F.L. Lewis, "Reinforcement adaptive learning neural-net-based friction compensation control for high speed and precision," *IEEE Transactions on Control System Technology*, vol. 8, no. 1, pp. 118-126, Jan. 2000.
- [8] K.O Sohn and T.Y Kuc, "Friction compensation of X-Y robot using a learning control technique," *Journal of Control, Automation and System Engineering*, vol. 6, no. 3,

Mar. 2000

- [9] S. Haykin, *A comprehensive Foundation Neural Networks*, Macmillan College Publishing Co., 1994.  
 [10] Y. Hujino and N. Kyura, *Practical Mechatronics Motion Control*, Industrial Publishing Co., Japan, 1996.



#### **Dae-Won Chung**

He was born in 1957. He received B.S. degree from Pusan University in 1983, M.S. and Ph.D. degrees in electrical engineering from Chungnam University in 1996 and 2000, respectively. From 1982 to 1996, he has been a senior researcher of Korea Atomic Energy

Research Institute. Since 1997, he has been a Professor at Department of Electrical Engineering, Honam University. His research interests are in the area of mechatronics servo systems, advanced and intelligent control techniques and digital microprocessor systems, etc.



#### **Nobuhiro Kyura**

He was born in 1942. He received B.S., M.S. and Ph.D. degrees in electrical engineering from Kyushu University in 1964, 1966 and 1992, respectively. From 1964 to 1995, he has been a general manager of the research laboratory of Yaskawa Electric

Corporation, Japan. Since 1995, he has been a Professor at Department of Electrical Computer Engineering, Kinki University in Kyushu. His research interests include motion controller architecture, optimum motion control and robot manipulator control, etc.



#### **Hiromu Gotanda**

He received the M.E. and D.E. degrees in electrical engineering from Kyushu University in 1978 and 1983, respectively. From 1986 to 1987, he was a Visiting Researcher at University of California at Berkeley. From 1981, he has been a Professor at Department of

Electrical and Computer Engineering, and is currently Dean and Professor of Graduate School of Advanced Technology, Kinki University in Kyushu. His research interests are in the areas of system theory, neural network, learning theory, signal processing, pattern recognition, speech information processing and speech recognition, etc.